Deep Semantic Hashing with Multi-Adversarial Training

Bingning Wang*
Institute of Automation, Chinese Academy of Sciences
bingning.wang@nlpr.ia.ac.cn

Kang Liu*
Institute of Automation, Chinese Academy of Sciences
kliu@nlpr.ia.ac.cn

Jun Zhao
Institute of Automation, Chinese Academy of Sciences
junz@nlpr.ia.ac.cn

ABSTRACT

With the amount of data has been rapidly growing over recent decades, binary hashing has became an attractive approach for fast search over large databases, in which the high-dimensional data such as image, video or text is mapped into a low-dimensional binary code. Searching in this hamming space is extremely efficient which is independent of the data size. A lot of methods have been proposed to learn this binary mapping. However, to make the binary codes conserves the input information, previous works mostly resort to mean squared error, which is proved to lose a lot of input information [11]. On the other hand, most of the previous works adopt the norm constraint or approximation on the hidden representation to make it as close as possible to binary, but the norm constraint is too strict that harms the expressiveness and flexibility of the code.

In this paper, to generate desirable binary codes, we introduce two adversarial training to the hashing process. We replace the L_2 reconstruction error with an adversarial training process to make the codes reserve its input information. And we apply another adversarial learning discriminator on the hidden codes to make the it proximate to binary. With the adversarial training process, the generated codes are getting close to binary while also conserves the input information. We conduct comprehensive experiments on both supervised and unsupervised hashing and achieves a new state of the arts result on many image hashing benchmarks.

CCS CONCEPTS

• **Computing methodologies** → *Neural networks*; • **Security and privacy** → *Hash functions and message authentication codes*;

KEYWORDS

Semantic Hashing; Generative adversarial network; Auto-encoder; Unsupervised Learning

ACM Reference Format:
Bingning Wang, Kang Liu[1], and Jun Zhao. 2018. Deep Semantic Hashing with Multi-Adversarial Training. In *The 27th ACM International Conference on Information and Knowledge Management (CIKM '18), October 22–26, 2018, Torino, Italy.* ACM, New York, NY, USA, 10 pages. https://doi.org/10.1145/3269206.3271735

*Bingning and Kang have equal contributions to this paper.

1 INTRODUCTION

Similarity search has many important applications such as document clustering, multimedia retrieval, and collaborative filtering [46]. In practical scenarios, especially when the data is very large, scalable retrieval is needed to accelerate the searching process. However, searching is very challenging since the feature space of data, such as images, usually span very high dimension. The operation such as calculating cosine distance in this high dimension is extremely computationally expensive, which requires a more efficient scheme for searching. To this end, semantic hashing, one of the most effective ways to accelerate the searching process through approximate matching based on binary code representation, has been widely studied and became the mainstream technique [14].

The basic idea of hashing is to map high dimensional data into low-dimension binary codes through a series of hash functions. Based on such binary representation, similarity could be efficiently calculated. Traditional methods for hashing such as locality-sensitive hashing (LSH) [5, 22], semantic hashing [39], spectral hashing [48] have been proved to be very useful for constructing such hash functions. However, they are either data-independent or requiring specific assumptions about the underlying distributions of the data, which hinder their applications in large-scale scenario [46].

Recently, with the renaissance of the neural networks in artificial intelligence, some deep learning based auto-encoder have been proposed for semantic hashing [3, 10, 32]. They usually adopt a neural network based encoder to embed the input $\mathbf{x}$ into a low-dimensional continuous hidden representation $\mathbf{h}$. And a decoder is used to build a reconstruction $\tilde{\mathbf{x}}$ from $\mathbf{h}$. As a result, $\mathbf{h}$ could be served as a surrogate of the input and used for hashing. Basically, these methods are based on two objectives: (I) the hidden representation $\mathbf{h}$ should preserve the semantic information of $\mathbf{x}$ as much as possible. (II) $\mathbf{h}$ should be as close as possible to binary.

In order to preserve the semantic information of input data, previous methods usually adopt norm constraint to make the reconstruction similar with the input, such as L_2 norm (mean squared error) or L_1 norm [3, 10]. The objective of reconstruction is $||\tilde{\mathbf{x}} - \mathbf{x}||_{1/2}$. However, it has been proved that simply employing the L_1 or L_2 norm is unable to capture the structure information of the input [12, 30], so the reconstruction is similar with the input only in a global view that loses a lot of details [11].

On the other hand, to approximate the hidden representations ($\mathbf{h}$) to binary codes, most previous approaches also adopt norm-constraint. For example, Binary Auto-encoders [3] use the L_2 norm to minimize the distance between $\mathbf{h}$ and its $sign$ value (i.e. $||sign(\mathbf{h}) - \mathbf{h}||_2$). However, the sign function is non-differentiable, it needs to be fine-tuned and become unstable when the code size is large [7]. To overcome such problem, some methods directly set a hard threshold to $\mathbf{h}$ to derive the binary codes [4, 47]. This strategy simplifies the optimization greatly but usually yield low-quality solutions [8].

In this paper, to generate better binary codes without any norm constraint, we propose a deep semantic hashing model based on generative adversarial networks (GANs) [17]. The whole architecture is based on an auto-encoder, which served as the generator in GANs. Then we use two discriminators as the adversarial components for the auto-encoder to learn the *distance* information, which bypasses the traditional norm constraints. We refer our model as **g**enerative **m**ulti-**a**dversarial **n**etworks (**GMANs**).

Specifically, to make the reconstruction of auto-encoder has more fidelity, we first use a discriminator to determine whether the input is *fake* (generated by the auto-encoder) or *real* (original input), and the output from such discriminator could be used as the distance information for training the auto-encoder. In this way, rather than employing the inefficient L_2 or L_1 loss, the auto-encoder is trained to minimize the Jensen-Shannon divergence as the reconstruction objective [17].

Secondly, we apply another discriminator to the hidden representation $\mathbf{h}$ of the auto-encoder to make $\mathbf{h}$ as close as possible to be binary. We randomly sample a binary code from a specified Bernoulli distribution and treat it as the *real* data for this discriminator. Meanwhile, the generated codes $\mathbf{h}$ are served as the *fake* data to the discriminator. In this case, the objective of the discriminator is to determine whether the input is binary or not. With such adversarial training, the generated codes from the auto-encoder are expected to get close to the real binary data.

Unfortunately, the GANs are notorious for training [40]. One of the most challenging problems is the mode collapse issue [42, 45]. Therefore, in this paper, we employ the variance of the generated codes as an additional regulator to train the generator, which could effectively alleviate the mode collapse problem. Besides, to make the adversarial training process more smooth and stable, we further propose a self-controlling scheme where the generator and discriminator are trained dynamically so that the generator could get the most substantial gradient from discriminator.

Our proposed model is based on auto-encoder which is purely unsupervised. However, it is straightforward to apply our model on a supervised scenario. We apply GMANs on the widely used image and text hashing datasets. Experimental results show the effectiveness of the proposed approach. We conduct further experiments to demonstrate the specific advantage of each adversarial network in our model. The results show that GMANs could yield better reconstructions compared with the previous method trained with the norm constraint. Moreover, the codes generated by GMANs could preserve the input information and are very close to binary. Although the proposed model is based on auto-encoder which is purely unsupervised, we further prove that it is straightforward to apply our model on supervised scenario. Briefly, the contributions of this paper can be summarized as follows:

- We proposed a novel semantic hashing model based on a generative multi-adversarial network. It uses two adversarial training to replace norm constraint to generate high-quality hashing codes.
- We proposed a variance control criteria and self-controlling training scheme on our GMANs to stabilize the training process.
- We conduct comprehensive experiments on several retrieval applications. The results show that our model achieves better results than state-of-the-art models on both supervised and unsupervised setups.

2 RELATED WORKS

Hashing has been regarded as an essential component in a variety of large-scale information retrieval systems. Locality-Sensitive Hashing (LSH) [22] is one of the most widely used unsupervised hashing methods with asymptotic theoretical properties of hashing guarantees. It constructs the hash functions based on many random linear projections. However, LSH is data-independent and usually requires many hashing bits to prevent the collision. To deal with this problem, several data-dependent hashing methods based on machine learning has been proposed. For example, Spectral Hashing (SpH) [48] explored the data distribution by preserving the similarity among the input data and adding the balanced and uncorrelated constraints into the learned codes. Iterative quantization [16] introduced structure and orthogonal constraints on the parameters, which could yield better results but also increase the computation complexity. Vector quantization and its generalizations [24, 52] constrained the binary representation to be 1-of-K coding, so that the corresponding optimization is simplified. However, with these extra constraints, the models become too restricted to generate proper binary codes and thus lose some important information of the inputs. Many deep learning based models have been proposed to reconstruct the data through an auto-encoder (AE). The hidden representation of the AE could be utilized as the hashing codes. Salakhutdinov and Hinton [39] proposed a deep learning model by using Restricted Boltzmann Machines (RBMs). This idea was then extended to more general auto-encoders which remove the Boltzmann constraints. For example, Liong et al. [33] proposed a model to learn the binary bits with auto-encoder jointly. However, there are too many norm constraints on the models which make the learning process extremely difficult to converge. Yu et al. [49] used circulant constraints and Zhang et al. [51] introduced Kronecker Product structure to achieve the binary constraints. These constraints could alleviate the convergence problem but substantially reduce the model flexibility. Other methods such as [7, 8] proposed some machine learning techniques to learn good hidden codes, but it necessitates the meticulous hyperparameter tuning. Chaidaroon and Fang [4] approximated a Gaussian prior on the hidden codes through variational inference. However, the Gaussian distribution is not appropriate for hashing applications where the desiderata of the codes are binary. Qiu et al. [38] is related to our model. They also proposed a GANs based hashing model. Their method is supervised where they use GANs to generate the *fake* image for pairwise learning. By contrast, the GANs in our model is introduced to the hashing process directly, which act as regulators, to make the latent code as binary as possible.

Generative Adversarial Networks GANs [17] is a recently proposed framework for estimating generative models via an adversarial process. In GANs, two types of models are simultaneously trained: a generator G is trained to estimate the data distribution and generate a fake sample; a discriminator D is trained to discriminate the real sample from the fake one. GANs corresponds to a minimax two-player game where there exists a unique solution that G recovers the data distribution, and D equals to $\frac{1}{2}$ everywhere. Many applications and improvement have been proposed to GANs, LAPGAN [9] generated images in a coarse-to-fine fashion by generating and upsampling in multiple steps; InfoGAN [6], an information-theoretic extension to the GANs that could learn disentangled representations. [50] extended the GANs to generating texts by policy gradient. WGAN [1] and BSGAN [21] were two typical ameliorations to vanilla GANs that had better training stabilities and theoretical advantages. Compared with other generative models such as variational auto-encoder [26], GANs could generate higher quality images without any distribution hypothesis. Thus it removes the inference process which is very hard to resolve in other generative models. The GANs have also shown advantages to replace or enhance the traditional metric-based methods in generative models. For example, Larsen et al. [30] found that the traditional L_1 or L_2 objective may cause the reconstruction be too blurred to be recognized. They also adopt the GANs on the learning process, but it was achieved based on a variational-auto-encoder. Dosovitskiy and Brox [11] extended their model by applying the GANs to the raw input. However, due to incomplete information, it must resort to L_1 or L_2 to learn the input-output correspondence. Most related method often adopts the adversarial learned inference [12], where the hidden state combined with the data is fed to the discriminator. However, their main motivation is to learn a better inference process. In this paper, our objective is to learn a better auto-encoder. Larsen et al. [30] also proposed a GANs framwork that contains more than one discriminator,but these discriminators are applied to the same output, i.e. the output of the generator. In this paper, the two discriminators are applied on different parts of the generator.

3 SEMANTIC HASHING WITH MULTI-ADVERSARIAL TRAINING

Our semantic hashing model is based on generative multi-adversarial networks. There is a generator which is built upon an auto-encoder. Two adversarial training processes are applied to the auto-encoder: the first one is an auto-encoder-GAN(AE-GAN) and the second one is a binary-GAN(B-GAN). AE-GAN is proposed to replace the traditional norm based reconstruction loss to make the hidden codes reserve the input information. B-GAN is proposed to make the generated codes approximate to binary.

We denote the raw input as $\mathbf{x}$, the generated hidden representation as $\mathbf{h} \in \mathbb{R}^b$, we use $\mathbf{h}$ as the hashing codes for the input. The conceptual architecture of GMANs is illustrated in Figure 1. In the following sections, we will refer the $\mathbf{h}$ as hidden representation or hidden codes interchangeably, next we detail the components of GMANs.

3.1 Generator

In GMANs the generator corresponds to the auto-encoder, which consists of two separate models, namely the encoder and decoder. The encoder e tries to embed the raw input $\mathbf{x}$ into a low-dimensional hidden representation $\mathbf{h}$ and the decoder f tries to decode $\mathbf{x}$ from $\mathbf{h}$:

$$\mathbf{h} = e(\mathbf{x}) \quad \tilde{\mathbf{x}} = f(\mathbf{h}) \tag{1}$$

We utilize the convolutional neural networks (CNNs) as the building block for our encoder. CNNs have shown great advantages in

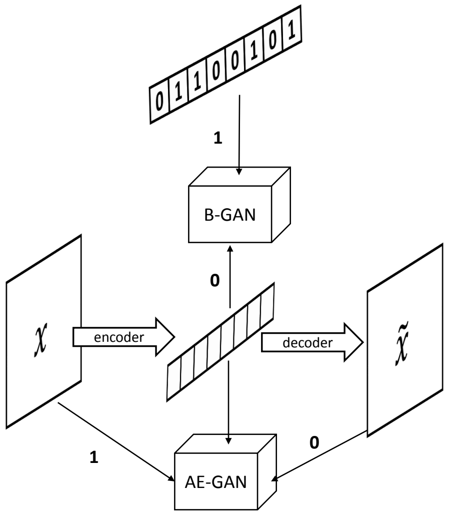

Figure 1: The architecture of the proposed model. 0 represents the fake data while 1 denotes the real data. The B-GAN tries to recognize whether the input is a binary (upmost) vector or a generated hidden codes. The AE-GAN tries to recognize whether the input is the real input (x) or generated (x̃). With the adversarial learning proceed, x̃ is more and more similar with x. Meanwhile the hidden representation is more approximate to be binary.

many applications [35, 43]. We convolute 5×5 filters $\mathbf{W}$ on the input, so the hidden representation of each layer could be denoted as:

$$\mathbf{h}_{i,j} = \text{Relu}(\mathbf{W} \otimes \mathbf{X}_{i-2:i+2,j-2:j+2} + \mathbf{b}) \tag{2}$$

where $\mathbf{b}$ is a bias vector. We did not adopt any pooling operation but apply CNN several times to the hidden representation to embed the input into a vector. The encoding process is illustrated below:

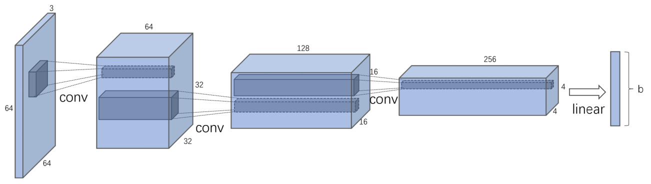

The decoder architecture can be viewed as the reversed process of the encoder. However, the CNN in the decoder is not the original convolutional operations but the transposed convolution[1] that maps the low-dimensional hidden representation to high-dimensional simulated data $\tilde{\mathbf{x}}$.

3.2 Auto-Encoder GAN

Traditional hashing methods based on auto-encoder often resort to the Euclidean distance between the input and output, which is more commonly referred as mean squared error, as the training objective:

$$\mathcal{L}_{rec} = d(\mathbf{x}, \tilde{\mathbf{x}}) = ||\mathbf{x} - \tilde{\mathbf{x}}||_2 \tag{3}$$

We call this objective as the norm loss. In AE-GAN, we replace this norm loss with an adversarial training loss. A discriminator in

[1] also known as stride-convolution or de-convolution.

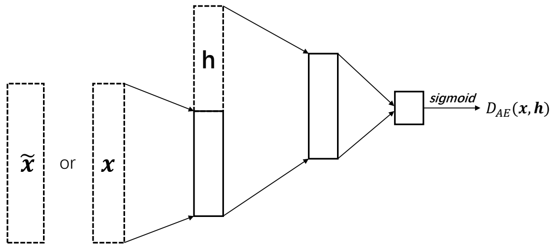

Figure 2: The architecture of D_{AE}. (1) The input has two parts: the hidden representation h of the auto-encoder, (2) the high-dimensional data x or its reconstruction $\tilde{\mathbf{x}}$. The output undergone a sigmoid function to clamped to [0,1].

AE-GAN tries to discriminate the original data $\mathbf{x}$ from the fake data $\tilde{\mathbf{x}}$ generated by the generator. So we can regard the discriminator as a metric function to provide *distance*[2] information.

In AE-GAN, the generator is the auto-encoder itself that tries to reconstruct the input. The discriminator in AE-GAN (denoted as D_{AE}) has two inputs: the first one is the hidden representation $\mathbf{h}$ of the generator, and the second one is the real or fake input ($\mathbf{x}$ or $\tilde{\mathbf{x}}$). The architecture of the D_{AE} is illustrated in Figure 2. During training, the objective of the D_{AE} is to minimize the probability of $\tilde{\mathbf{x}}$ while increase the probability of $\mathbf{x}$, which can be denoted as:

$$\begin{aligned}\mathcal{L}_D^{AE} &= -\mathbb{E}_{\mathbf{x}\sim p(x),\mathbf{h}=e(\mathbf{x})}[\log D_{AE}(\mathbf{x},\mathbf{h})] \\ &\quad - \mathbb{E}_{\mathbf{x}\sim p(x),\mathbf{h}=e(\mathbf{x}),\tilde{\mathbf{x}}=f(\mathbf{h})}[\log(1-D_{AE}(\tilde{\mathbf{x}},\mathbf{h}))]\end{aligned} \tag{4}$$

$p(x)$ is the data empirical distribution. In this manner, we could use the output of D_{AE} as the objective for the generator to optimize. The objective of the generator is:

$$\mathcal{L}_G^{AE} = -\mathbb{E}_{\mathbf{x}\sim p(x),\mathbf{h}=e(\mathbf{x}),\tilde{\mathbf{x}}=f(\mathbf{h})}[\log D_{AE}(\tilde{\mathbf{x}},\mathbf{h})] \tag{5}$$

This objective is minimized only when the reconstructed $\tilde{\mathbf{x}}$ match the original input $\mathbf{x}$. However, in practice, the discriminator is a two-class classifier, so it prone to get too far ahead. Because the discriminator's output is sigmoidal that the gradient of the value function with respect to the discriminator's output vanishes to zeros, the generator may have a hard time minimizing the value function above. As a workaround, we train the generator of AE-GAN similar with [12] that maximize:

$$\begin{aligned}\mathcal{L}_G^{AE} &= -\mathbb{E}_{\mathbf{x}\sim p(x),\mathbf{h}=e(\mathbf{x})}[\log(1-D_{AE}(\mathbf{x},\mathbf{h}))] \\ &\quad - \mathbb{E}_{\mathbf{x}\sim p(x),\mathbf{h}=e(\mathbf{x}),\tilde{\mathbf{x}}=f(\mathbf{h})}[\log D_{AE}(\tilde{\mathbf{x}},\mathbf{h})]\end{aligned} \tag{6}$$

With the training proceed, the reconstruction $\tilde{\mathbf{x}}$ could be more and more similar with the input $\mathbf{x}$ at the guidance of discriminator D_{AE}.

3.3 Binary GAN

While the AE-GAN focuses on minimizing the reconstruction error, the objective of the B-GAN is to approximate the hidden representation into binary codes that could be utilized for hashing. Similar to the AE-GAN, the generator in the B-GANs corresponds to the auto-encoder itself [3]. Denote the discriminator in B-GAN as D_B. We use a multi-layer perceptron (MLP) as the building block for D_B. In this paper, we adopt scaled exponential linear units (SELU) [27] as the activation function for D_B:

$$g(x) = \gamma \begin{cases} x & if \quad x > 0 \\ \alpha e^x - \alpha & if \quad x \le 0 \end{cases} \tag{7}$$

Where the γ and α are two hyper-parameters of SELU. The SELU shows advantage in convergent speed of the MLP compared with other activation functions such as $Tanh$ or $Relu$.

For B-GAN, the preferred input is the binary codes, so the real input to D_B is a binary vector drawn from a Bernoulli distribution:

$$\mathbf{b} \sim B(b, p) \tag{8}$$

where b is the number of the bits to be sampled and p is the probability that corresponding bit being 1. Previous works on hashing usually assume the balanced bit, so it is trivial to set p to 0.5 which means half of the bits to be fired, but we can set p to any value between 0 and 1 for different applications. D_B acts as a critic that output higher score when the input is closer to binary. As the adversarial opponents, the generator has to generate more binary codes to achieve a higher score. Similar to AE-GAN, the objective for B-GAN can be denoted as:

$$\begin{aligned}\mathcal{L}_D^{B} &= -\mathbb{E}_{\mathbf{b}\sim B(b,p)}[\log D_B(\mathbf{b})] \\ &\quad - \mathbb{E}_{\mathbf{x}\sim p(x),\mathbf{h}=e(\mathbf{x})}[\log(1-D_B(\mathbf{h}))] \\ \mathcal{L}_G^{B} &= -\mathbb{E}_{\mathbf{x}\sim p(x),\mathbf{h}=e(\mathbf{x})}[\log D_B(\mathbf{h})]\end{aligned} \tag{9}$$

Thus $\mathcal{L}_G^B$ is minimized only when h is binary. However, using Equation 9 to train the generator may be problematic. The real input is binary vector, so the difference between the real and fake input is trivial to be discriminated. In other words, it is unlikely that the model manifold and the true Bernoulli distribution's support have a non-negligible intersection. To alleviate this problem, we add a

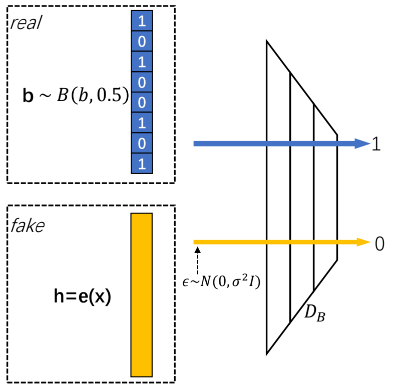

Figure 3: The architecture of D_B. The input could be either the generated codes h from auto-encoder (orange) or random sampled binary codes b (blue).

[2] More mathematically. It could be regarded as the divergence between the distribution supported by data manifold and the density of the generator. The original GANs[17] cast it as Jensen-Shannon divergence while some other works [37] extended this to more general f-divergences.

[3] Although we can use the output of auto-encoder as the input for the generator to generate the binary code, it has a trivial difference with the proposed strategy. The generator has already involved in the auto-encoder, so we use the auto-encoder as the generator.

noise term to the model distribution. In this case, the fake examples fed to D_B could be formulated as:

$$\mathbf{h}' = e(\mathbf{x}) + \epsilon, \quad \epsilon \sim \mathcal{N}(0, \sigma^2 \mathbf{I}) \tag{10}$$

Where σ is the standard deviation of the Gaussian noise which was set to 0.1 in the experiment. The main difference is that we will move our generated codes towards the noised data manifold, which can be thought of as transfer a small neighbourhood of samples towards it. This will protect the discriminator against measure zero adversarial examples, and thus push the generator towards a better manifold. More importantly, the gradient of the generator would correspond with the original one (i.e. two times derivative of the Jensen-Shannon divergence)[1]. The architecture of B-GAN is illustrated in Figure 3.

3.4 Mode Collapse Elimination

In experiments, we observe that the B-GAN is prone to mode collapse problem, in which the generated codes collapse to few points that are very similar to binary. Thus the binary score of the generated codes $D_B(\mathbf{h})$ is very high, but the variance of different codes is very small. In another word, no matter what the input is, their corresponding codes generated by the auto-encoder is very close to each other. In theory, this problem is attributed to the fact that the minor mode of the data seldom (approaches to zero probability) getting reward from the discriminator. To eliminate this problem, we add another criterion to the auto-encoder to control the variance of the generated codes:

$$\mathcal{L}_V = \mathbb{E}_{\mathbf{B},\mathbf{H}}[(Var(\mathbf{B}) - Var(\mathbf{H}))^2] \tag{11}$$

where $\mathbf{B}$ and $\mathbf{H}$ are batch of real binary codes and generated representations respectively. The variance of the code is:

$$Var(\mathbf{H}) = trace(\mathbf{H}^T\mathbf{H}) \tag{12}$$

As we sampled the real binary vector randomly and independently, we can trivially set $Var(\mathbf{B})$ to mb where m is the batch size. In this way, the generated codes would be as variable as the sampled binary codes, and could somewhat bypass the mode collapse problem. Adding the variance loss to the original loss we get the final objective of the generator (auto-encoder):

$$\mathcal{L}_G = \lambda_1 \cdot \mathcal{L}_G^{AE} + \lambda_2 \cdot \mathcal{L}_G^{B} + \lambda_3 \cdot \mathcal{L}_V \tag{13}$$

where $\lambda_{1,2,3}$ are three hyper parameters to determine the weight of each objective in training.

3.5 Self-Controlled Training procedure

Previous works of GANs carry the adversarial training process under a situation of *nearly-perfect* discriminator, so they update the discriminator more often than the generator[4] which is claimed to push the generator to the optimal region. However, we find that this mechanism would lead to unstable training process. If the discriminator gets to its optimal situation that it could correctly discriminate the real from the fake data, then the output from the discriminator lies in the saturated region of the sigmoid, so the gradient of from the discriminator to the generator has a large variance. Such high variance may seriously infect the training process and make the generator hardly, if not impossible, to be optimized.

[4]Most previous works updated the discriminator 5 times while only update the generator once in each step.

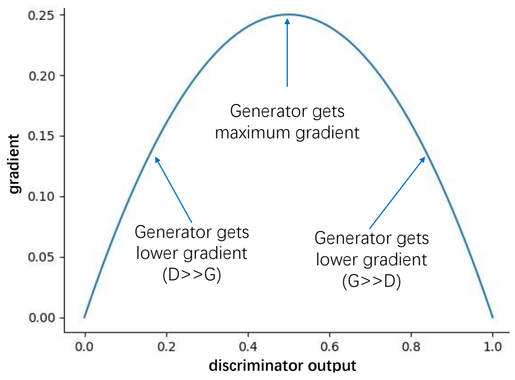

Figure 4: The gradient of the discriminator w.r.t. its output. If the output value larger than 0.5, which denotes the generator (G) overtake the discriminator (D), and when the output value smaller than 0.5, G falls behind the D.

In this paper, to make the generator get gradient from the discriminator consistently, we proposed a training strategy where the generator is updated at the *best guidance* of the discriminator, i.e. the generator could get the largest gradient from the discriminator. Remember that the gradient of the sigmoid function is: $f'(x) = f(x) \cdot (1 - f(x))$, so it peaks on the value of 0.5. When the output value of discriminator is larger or smaller than 0.5, then it's gradient will decrease. The gradient of the discriminator could be illustrated in Figure 4.

Algorithm 1 Deep Semantic Hashing with Generative Multi-Adversarial Networks

```
Require: weight for each objective $\lambda_{1,2,3}$ and fixed learning rate $\lambda$ .
 1: Pre-training auto-encoder by Equation 3.
 2: for number of training iterations do
 3:     Random sample a training data $\mathbf{x}$.
 4:     Calculate $\mathbf{h}$ and $\tilde{\mathbf{x}}$ from Equation 1.
 5:     if $D_{AE}(\tilde{\mathbf{x}}, \mathbf{h}) > 0.5$ then
 6:         Calculate $\mathcal{L}_D^{AE}$ using Equation 4.
 7:         ▷ Update the discriminator of AE-GAN:
 8:         $\nabla_{\theta_D^{AE}} = \frac{d_{\mathcal{L}_D^{AE}}}{d_{\theta_D^{AE}}} \quad \theta_D^{AE} = \theta_D^{AE} + \lambda \nabla_{\theta_D^{AE}}$
 9:     if $D_B(\mathbf{h}) > 0.5$ then
10:         Calculate $\mathcal{L}_D^B$ using Equation 9.
11:         ▷ Update the discriminator of B-GAN:
12:         $\nabla_{\theta_D^B} = \frac{d_{\mathcal{L}_D^B}}{d_{\theta_D^B}} \quad \theta_D^B = \theta_D^B + \lambda \nabla_{\theta_D^B}$
13:     Calculate $\mathcal{L}_G^{AE}$, $\mathcal{L}_G^B$ and $\mathcal{L}_V$ using Equation 5,9 and 11.
14:     $\mathcal{L}_G = \lambda_1 \cdot \mathcal{L}_G^{AE} + \lambda_2 \cdot \mathcal{L}_G^B + \lambda_3 \cdot \mathcal{L}_V$
15:     ▷ Update the generator (auto-encoder):
16:     $\nabla_{\theta_G} = \frac{d_{\mathcal{L}_G}}{d_{\theta_G}} \quad \theta_G = \theta_G + \lambda \nabla_{\theta_G}$
```

To keep the discriminator at the best situation that could provide good gradient for the generator, we just utilize the score of the fake example $D(\mathbf{h})$ or $D_{AE}(\tilde{\mathbf{x}}, \mathbf{h})$ to determine whether we should train the

	CIFAR10					MNIST					SIFT1M				
b	8	16	24	32	48	8	16	24	32	48	8	16	24	32	48
SH [48]	0.39	4.23	14.37	15.12	16.23	0.44	6.51	27.08	36.69	39.22	3.67	15.32	27.25	32.40	42.23
ITQ [16]	0.51	5.21	17.77	17.46	16.99	0.51	5.87	23.92	36.35	38.99	5.18	19.23	30.15	46.23	48.22
SPH [20]	0.43	3.45	13.47	14.67	15.23	0.44	5.02	22.24	30.80	33.29	2.25	18.98	31.09	44.42	51.26
KMH [18]	0.53	5.49	19.55	15.90	14.58	0.50	6.36	25.68	36.24	36.77	3.74	19.85	28.86	46.04	52.28
BA [3]	0.55	5.65	20.23	17.00	16.35	0.51	6.44	27.65	35.29	34.28	3.18	19.35	22.42	40.28	50.85
BDNN [10]	0.55	5.79	22.14	18.35	20.28	0.53	6.80	29.38	38.50	37.48	3.75	18.96	33.83	48.12	53.39
VDSH [4]	0.61	5.99	23.41	19.17	21.05	**0.55**	6.99	25.36	38.12	36.28	3.99	18.96	33.10	46.82	52.36
w/o AE-GAN	0.59	5.87	22.18	18.81	20.79	0.51	5.91	28.76	37.99	35.78	3.99	19.21	33.52	48.95	53.98
w/o B-GAN	0.56	5.89	23.38	18.95	21.70	0.52	5.99	27.98	38.21	36.03	4.01	18.52	30.19	46.36	52.74
GMANs	**0.62**	**6.06**	**25.25**	**20.17**	**22.86**	0.53	**7.35**	**30.26**	**40.26**	**39.32**	**4.04**	**19.98**	**34.26**	**50.16**	**55.39**

Table 1: Precision at hamming distance less than 2 on several image datasets.

	RCV1				20Newsgroups		
b	8	16	32	64	8	16	32
SH [48]	42.71	55.22	72.36	48.46	14.37	23.67	41.00
SPH [20]	44.31	65.26	68.17	47.90	12.41	26.12	29.38
BA [3]	73.87	75.32	82.83	81.67	15.18	42.23	39.13
BDNN [10]	75.38	81.52	83.31	75.90	18.44	41.56	43.61
VDSH [4]	71.32	83.99	83.01	79.12	22.46	46.84	40.29
w/o AE-GAN	77.35	84.46	83.77	78.03	23.18	47.22	44.01
w/o B-GAN	75.07	82.98	83.38	78.91	23.09	46.51	43.82
GMANs	**79.31**	**85.17**	**84.76**	**83.81**	**23.23**	**47.93**	**44.59**

Table 2: Precision at hamming distance less than 2 on several text datasets. For 20Newsgroups as the data size is comparatively small, so we did not experiment with code length 64.

generator or discriminator. When the fake data score is larger than 0.5, we train the discriminator. Otherwise, the generator is trained. From this self-controlled process, the generator and the discriminator could be improved synchronously. The overall training process of GMANs is illustrated in Algorithm 1.

4 EXPERIMENTS

In this section, we show the overall results of our GMANs on several images and textual retrieval tasks. In the next section, we will make a detailed analysis of the advantages of the proposed model.

4.1 GMANs vs. State-of-the-arts

4.1.1 ***Datasets.*** We apply the GMANs to three image datasets and two text datasets that are widely used as the unsupervised benchmarks for semantic hashing [46]. The image datasets include:

- **CIFAR10** [28]: a dataset of 32x32 color images, each images contains one of ten objects. The training set contains 50k images, and the query (testing) set contains 10k images. We use the training set as the retrieval set.
- **MNIST** [31]: It contains 70k handwritten digit images of 10 classes. The training set contains 60k images and the testing set contains 10k images. Each image is a 28x28 greyscale matrix. We use the 60k training set as the retrieval set.
- **SIFT1M** [24]: It contains 128-d SIFT [34] descriptors. The training set contains 100k images and there are 10k vectors for testing. We use the provided 1m images as the retrieval set.

Moreover, we select the following two text classification datasets to evaluate our model, which have been widely adopted in previous works [4, 39]:

- Reuters Corpus Volume I (**RCV1**): A large collection of manually labelled 800k newswire stories provided by Reuters with totally 103 classes. We use the full-topics version that had been transformed to LIBSVM format[5].
- **20Newsgroups**: It is a collection of 18,828 newsgroup posts that have been partitioned across 20 categories. We select the popular byte-data and use the stemmed version[6] pre-processed by Ana Cardoso-Cachopo [2]. We further truncate the length of the text to 300.

4.1.2 ***Experimental Settings.*** For CIFAR10 and MNIST, as the input is raw images, we use the CNN with stride size 2 as the building block for auto-encoder. For SIFT1M, the input is the hand-crafted SIFT [34] features, so we use the MLP for the auto-encoder, which is similar to the setting in the compared baselines. For CNN architecture, we initialize all the weight parameters by MSRA [19]: an extension to Xavier and suited for ResNet setting. Batch normalization [23] is added to the encoder and decoder CNN layer to accelerate the training process. For MLP, we initialize their weights by Xavier [15]. We train our model based on Adam [25] algorithms. Batch size is set to 16 for CIFAR10 and MNIST, 32 for SIFT1M. For MLP, the layer size L is set to 3 for both encoder and decoder. λ_1 λ_2 is set to 0.2 and 0.5 respectively. For all setup, we set the code length (i.e. b) to be 8, 16, 24, 32 and 48, respectively.

For the text data, as the input is the tf-idf features, we build the GMANs based on MLP, the hidden layer size is halved every layer from 128 to 32. As the input size is relatively large (vocab size was set to 2000), we gradually increasing λ_1, λ_2 from 0 to 0.1, which means that we first learn a good auto-encoder and then impose the binary constraint on it.

4.1.3 ***Evaluation Metrics.*** For image hashing evaluation, we follow the standard setting in unsupervised hashing that used Euclidean space nearest neighbors of each query as the ground truths

[5]https://github.com/JohnLangford/vowpal_wabbit/wiki/Rcv1-example
[6]http://web.ist.utl.pt/acardoso/datasets/

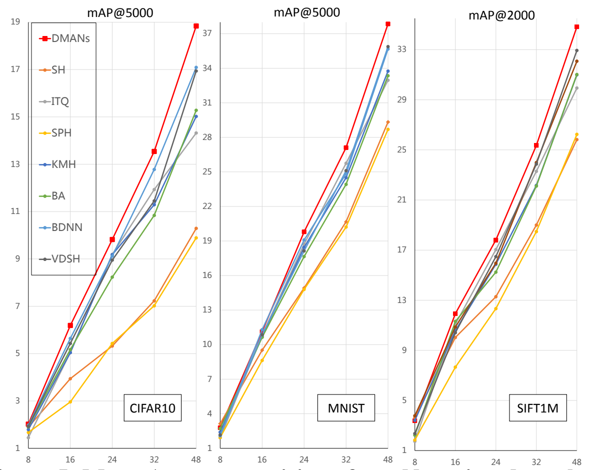

Figure 5: Mean Average precision of top-N retrieved results on several image datasets. For SIFT1m we set N to 2000 as it has relatively large size. X-axis is the code length.

[3, 10, 46]. For CIFAR10 and MNIST datasets, we use 50 Euclidean nearest neighbors as the ground truths. For SIFT1M we use 5000 Euclidean nearest neighbors as the ground truths. For the document data, the ground truths documents are those that share the same label with the query document.

We adopt three widely used metrics for evaluation: 1) mean Average Precision of top N retrieved item (**mAP@N**); 2) precision of Hamming radius 2 (**precision@2-bit**). It measures precision on retrieved images having Hamming distance to query less than 2 (if no images satisfy we set it to zero); 3) Precision of top N (**P@N**) retrieved items, which measures whether the system could retrieve the ground-truth items in the top-N retrieved items. We apply mAP@N to image and P@N to text, precision@2-bit is evaluated on both text and image. All experiments have been gone through the significant test, i.e., one-tailed paired t-test with a default 95% significance level is used here.

4.1.4 ***Baselines***. We compare GMANs with seven competitive baselines which have been extensively used for unsupervised semantic hashing, including: Spectral Hashing (**SH**) [48], Iterative Quantization (**ITQ**) [16], Spherical Hashing (**SPH**) [20], K-means hashing (**KMH**) [18], Binary Auto-encoder (**BA**) [3], Binary Deep Neural Network (**BDNN**) [10], Variational deep semantic hashing (**VDSH**) [4]. In addition, to make specific comparison, we also conduct several ablation studies where we: (1) minimizing the reconstruction error by L_2 instead of the AE-GAN (**w/o AE-GAN**) (2) Optimizing the hidden codes to their corresponding binary vector by L_2 norm constraints (**w/o B-GAN**).

The result is shown in Table 1, 2 and Figure 5 and 6.

4.2 Main Results

It could be seen from table 1, 2 and figure 5, 6 that our proposed GMANs consistently outperform previous methods. Especially, from figure 5 we could observe that the advantage is more significant when the code length increase. This is attributed to the fact that when the code length (i.e. the hidden representation size) is large, it becomes more and more difficult for traditional norm constraint

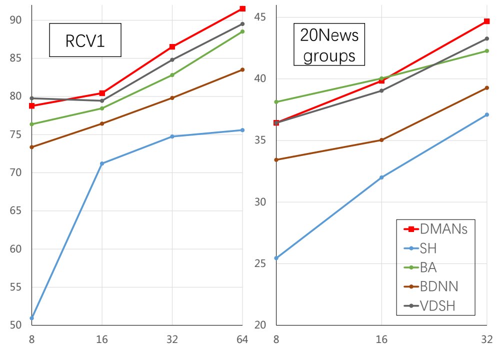

Figure 6: Precision@200 for RCV1 and 20Newsgoups.

to optimize the hidden codes [46]. However, in our GMANs, the distance information is provided by the discriminator which is less vulnerable to the increasing code length.

The ablation study in table 1 and 2 shows that our proposed adversarial training strategy outperforms the traditional models based on norm constraint. For example, in CIFAR10, the performance of the model without AE-GAN drops a lot. The input in CIFAR10 is 32*32 colored image which lies in high space, so the reconstruction by L_2 norm in Equation 3 may put no attention on the specific area of the input. On the contrary, our model utilizes deep neural networks to measure this distance, which would capture more important information of the input image. In addition, the model without B-GAN behaves poorly. We find in the experiment that when using the norm loss $||sign(\mathbf{h}) - \mathbf{h}||_2$ to optimize the hidden code, the auto-encoder became very hard to be optimized, and the generated codes quickly collapse to some point. Thus in some previous works, they also add extra regulation terms to prevent the collapse, such as the orthogonality regulation on projection matrix [13]. By contrast, our model alleviates this optimization difficulty by the two discriminators, which is more flexible and achieves better results.

5 ANALYSIS

5.1 The Advantage of AE-GAN

In this subsection, we try to prove that the proposed AE-GAN could reconstruct the input with better fidelity. However, evaluating the quality of synthesized images is an open difficult problem [40]. In the auto-encoder setting, the output lies on continues feature space, so the *likelihood* of the generated image is difficult to calculate. Traditional metrics such as per-pixel Euclidean distance do not assess joint statistics of the result, and therefore do not measure the very structure and information that we want to capture in the input.

Some recent works [1, 12, 36] have tried to use pre-trained image semantic classifiers to measure the quality of the generated stimuli as a pseudo-metric. The intuition is that if the generated images are realistic, classifiers trained on real images will be able to identify the synthesized image correctly as well. Similar to them, we adopt a popular Inception[7] [44] model. For the input $\mathbf{x}$, the output of the Inception could be denoted as $p(\mathbf{y}|\mathbf{x})$ that corresponding to the distributions of the input categories, and $p(\tilde{\mathbf{y}}|\tilde{\mathbf{x}})$ is the output distribution

[7]We use the off-the-shelf public Inception-v3 model from https://download.pytorch.org/models/inception_v3_google-1a9a5a14.pth.

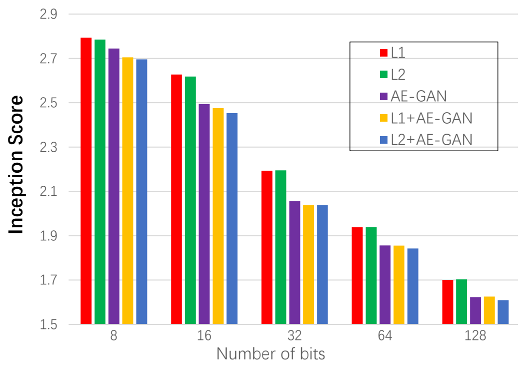

Figure 7: Inception score of the different loss for auto-encoder. The lower the better. Best viewed in color.

of generated image $\tilde{\mathbf{x}}$ going through the Inception model. Then we can use the divergence between $p(\mathbf{y}|\mathbf{x})$ and $p(\tilde{\mathbf{y}}|\tilde{\mathbf{x}})$ to evaluate the quality of the reconstructed image, which is referred as the Inception score:

$$\mathbb{E}_{\mathbf{x}}(\mathrm{KL}(p(\mathbf{y}|\mathbf{x})||p(\tilde{\mathbf{y}}|\tilde{\mathbf{x}}))) = \sum_{\mathbf{x}}\sum_{i}^{L} p(\mathbf{y}_i|\mathbf{x}) \log \frac{p(\mathbf{y}_i|\mathbf{x})}{p(\tilde{\mathbf{y}}_i|\tilde{\mathbf{x}})} \tag{14}$$

Thus if the reconstructed image is more similar to the input, the Inception score will be lower. For this comparison, we conduct the experiment on ILSVRC2012 dataset with 1,000 categories. We select two baselines for comparison, namely L1 and L2. L1 minimize the reconstruction error by $|\mathbf{x} - \tilde{\mathbf{x}}|$ and L2 minimize the reconstruction error by Equation 3. The Inception score compared with different auto-encoder objective is shown in Figure 7.

It could be seen from the figure that AE-GAN performs better than the L_1 or L_2 loss. Besides, when the AE-GAN is pre-trained with traditional L_2 objective (L2+AE-GAN), our model obtains the best Inception score. We think the reason is: the objective of the auto-encoder is to encode the information of the input, however, the objective of traditional L_1 or L_2 norm loss is to minimize the summation of per-pixel feature distance, which results in a reconstructed image that looks similar with the input only at a *global* view. In AE-GAN the distance metric is measured by a deep neural network (discriminator). Thus it is flexible to capture both global and local information of the input [12, 30]. We plot some examples in Figure 8, and we can see that the reconstruction by L_1 or L_2 loses a lot of details. By contrast, in the AE-GAN the reconstruction is more clear.

5.2 Advantage of B-GAN

Another contribution of the proposed methods is to approximate the binarization by introducing the adversarial objective $\mathcal{L}_G$. On the contrary, most previous methods [3, 10, 13] apply the norm constraint on the hidden codes to make it approximate to binary:

$$\mathcal{L}_b = ||sign(\mathbf{H}) - \mathbf{H}||_2 \tag{15}$$

where $\mathbf{H}$ is the hidden codes and *sign* function maps the input to ± 1.

In order to compare $\mathcal{L}_G$ and $\mathcal{L}_b$ quantitatively, inspired by Precision-Recall curve in the evaluation of traditional information retrieval tasks, we proposed the **Fidelity-Binarization (F-B)** curves. The fidelity could be the similarity between the input and output, and the

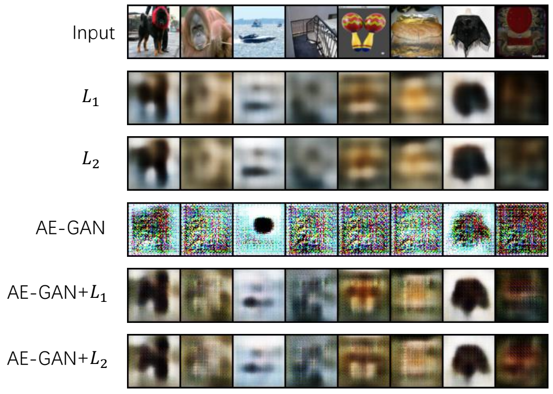

Figure 8: Reconstruction samples with different training criteria. L_1 or L_2 result in too blurred images that lose a lot of edge information, while only using AE-GAN will generate unrealistic images. Combine the norm constraint and AE-GAN together yield best results.

binarization could be regarded as the distance between the hidden codes and its binary vector. The two metrics are opponent just like the precision and recall: If we want to increase the fidelity, we must relax the binary constraint on the hidden codes and vice versa. Fidelity could be calculated by the L_2 distance between reconstruction and the input. To evaluate the binarization property, we consider three aspects of the hidden codes:

$$\begin{aligned} b_1 &= -\log(\frac{1}{nb}\sum_{i=1}^{n}\sum_{j=1}^{b}(1 - |\mathbf{H}_{ij}|)^2) \\ b_2 &= -\log(\frac{1}{nb} trace(\mathbf{H}^T \cdot \mathbf{H})) \\ b_3 &= -\log(\frac{1}{n}|\mathbf{H}^T \cdot \mathbf{1}|) \end{aligned} \tag{16}$$

where n is the data size and b is the code length. The b_1 considers hidden codes approximation to binary. b_2 considers the independence of the hidden codes, and the b_3 considers the balance of the codes, which is equal to the proportion of the hidden codes to be fired. These three metrics has been adopted as the training criteria in some previous works [20, 33]. As the elements of $\mathbf{H}$ lies in $(-1, 1)$, there exist upper bound for the three metrics. We use this upper bound to normalize the three term to restrict each of them to $[0, 1]$ (b_1', b_2', b_3'), and then combine this three metrics linearly to form the quality of the binarization.

$$binarization = b_1' + b_2' + b_3' \tag{17}$$

As the only focus of this section is to measure the improvement of B-GAN, we adopt the L_2 norm loss as the reconstruction objective. Thus the overall object could be formulated as:

$$\mathcal{L} = \beta \cdot \mathcal{L}_{rec} + (1 - \beta) \cdot \mathcal{L}_{binary} \tag{18}$$

where $\mathcal{L}_{binary}$ denotes $\mathcal{L}_G$ or $\mathcal{L}_b$. β is the weight of the two objective. When we set β to 1, we only minimize the reconstruction error, and setting it to 0 means we only optimize the binarization. Tuning this weight we can plot the binarization curve at different fidelity value. We use the CIFAR10 dataset and tuning the hidden codes size from 32 to 256, the results are shown in Figure 9.

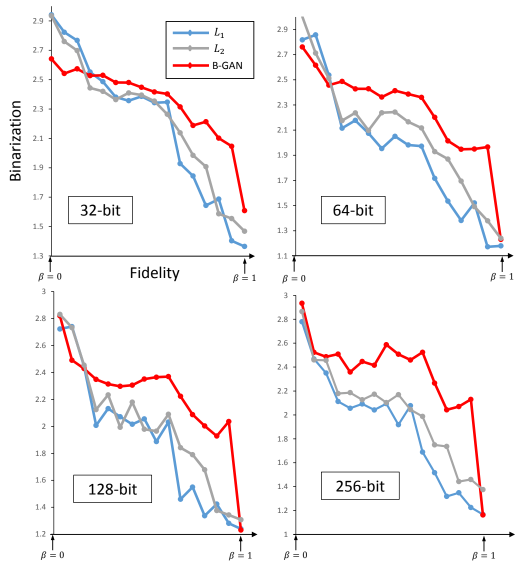

Figure 9: F-B curve for different bits on CIFAR10. The X-axis is the reconstruction value that has been normalized to [0,1]. $\beta = 0$ means we only optimize for binary loss, $\beta = 1$ means we only optimize the reconstruction loss. L_2 refers to Equation 15 and L_1 replace the Euclidean norm with L_1 distance.

It could be seen from the figure that our proposed model could achieve a better result than traditional L_1 or L_2 loss. To minimize the reconstruction error, the model with norm constraints has to sacrifice the binarization to obtain good fidelity. As a result, when we increase the weight of fidelity, the binarization curves drop quickly. For the proposed model, the binarization error stays relatively stable, which means our model could reduce the reconstruction error and binarization error simultaneously and efficiently. The advantage of our model is more significant when the code length increase. In the experiment, we found that the gradient of the L_1 or L_2 became unstable with the code length increasing, and requires a meticulous hyper-parameter calibration. By contrast, in GMANs we relax the norm constraint with the GAN and the binarization is achieved by reducing discriminator error, so it is relatively insensitive to the code length. This demonstrates the advantage of applying adversarial training for hidden codes generation.

5.3 GMANs on Supervised Setting

The proposed model is based on unsupervised setting, and it could be trivially extended to the supervised scenario. In the supervised setting, not only the raw-sample but also the corresponding labels are given, such as the data category, pairwise distance etc. Image similarity in the original feature space may not fully reflect the semantic relationship between them, and it has been revealed that the extra labels could enrich the semantic capacity of the auto-encoder based hashing model [3, 4, 10].

In this paper, suppose the label or tag information associated with the input $\mathbf{x}$ is $\mathbf{y}$, which is a one-hot vector indicating the class of the input. Similar with previous works on semantic hashing that utilizing the label information [4, 10], we build a classifier on the hidden representation $\mathbf{h}$. The classifier is based on MLP and we adopt the cross-entropy to optimize the classifier:

$$\tilde{\mathbf{h}} = MLP(\mathbf{h})$$
$$\tilde{\mathbf{y}} = Softmax(\tilde{\mathbf{h}}) \tag{19}$$
$$\mathcal{L}_S = -\sum_{j=1}^{C} \mathbf{y}_j \cdot \log \tilde{\mathbf{y}}_j$$

where C is the number of classes. Adding this term to Equation 13 we obtain the supervised objective of the generator:

$$\mathcal{L}_{G+s} = \lambda_1 \cdot \mathcal{L}_G^{AE} + \lambda_2 \cdot \mathcal{L}_G^{B} + \lambda_3 \cdot \mathcal{L}_V + \lambda_4 \cdot \mathcal{L}_S \tag{20}$$

where λ_4 is the parameter to tune the weight of the classifier.

Similar to the unsupervised setting, we apply the supervised GMANs (SGMANs) on two images and two texts datasets: 1) CIFAR10; 2)MNIST; 3) RCV1; 4) 20Newsgroups. For the supervised weight λ_4 in Equation 20, we gradually increase it from 0 to 1, which means we first learn a good auto-encoder and then embed the label supervision into the learning process. For all setups, the classifier is a two-layer MLP with hidden size equal to 64. We adopt four supervised hashing models for comparison. 1) Supervised Discrete Hashing (SDH) [41]. 2) Binary Reconstructive Embedding (BRE) [29]. 3) BDNN [10]. 4) Supervised VDSH (SVDSH) [4]. For all datasets, we evaluate the SGMANs by precision@2. The result is shown in Table 3.

	CIFAR10			MNIST		
d	8	16	32	8	16	32
SDH [41]	31.60	62.23	67.63	36.49	93.00	94.11
BRE [29]	23.84	41.11	44.89	37.67	69.80	84.61
BDNN [10]	54.12	67.32	69.62	84.26	94.67	94.52
SVDSH [4]	45.41	59.59	69.18	55.43	92.48	95.01
SGMANs	**58.48**	**69.20**	**69.75**	**85.91**	**95.81**	**96.33**
	RCV1			20newsgoup		
d	8	16	32	8	16	32
SDH [41]	53.31	82.39	79.54	28.44	37.73	39.51
BRE [29]	49.34	88.48	85.32	30.18	52.89	55.48
BDNN [10]	51.45	89.45	88.18	32.59	61.45	66.43
SVDSH [4]	**80.45**	96.48	90.28	30.58	65.32	69.18
SGMANs	77.85	**96.56**	**92.54**	**34.38**	**68.28**	**70.43**

Table 3: Supervised results of Precision at hamming distance less than 2.

We can see from table 3 that similar with the unsupervised application, our proposed GMANs also excels on supervised setting. The extra label information is embedded to the hashing process, and dynamically tuning the training process of hidden representation. Compared to unsupervised result in table 1 and 2, the supervised model could obtain higher precision on the retrieval task, which confirms the previous observation that the semantic information is important for hashing [3, 4, 10]. In addition, different from previous methods such as SDH [41] or Deep-SDH [32] that directly utilize the label for training, our model treat the label as an additional criterion in Equation 20, which is more flexible to apply.

6 CONCLUSION

In this paper, we proposed a deep semantic hashing model based on multiple adversarial training. The proposed architecture is based on auto-encoder, however, different from previous methods that using L_1 or L_2 norm constraint, we use two GANs to optimize the generated codes to make it as close as possible to binary and conserves the input information. Furthermore, we proposed a variance control method to eliminate the mode collapse problem and design a self-controlled mechanism to stabilize the training process of GANs. Several supervised and unsupervised experiments in text and image datasets reveal the advantage of the proposed GMANs. In addition, we do a comprehensive analysis to show the advantage of the two adversarial training process of the proposed model. In the future, we want to extend the GMANs to other hashing models rather than auto-encoder to improve the generated codes.

7 ACKNOWLEDGEMENTS

The research work was supported by the National Science Foundation of China (No. 61533018, 61702512). This work was also supported by a grant from Ant Financial Services Group and supported by the independent research project of National Laboratory of Pattern Recognition.

REFERENCES

[1] Martín Arjovsky, Soumith Chintala, and Léon Bottou. 2017. Wasserstein GAN. *CoRR* abs/1701.07875 (2017).
[2] Ana Margarida de Jesus Cardoso Cachopo. 2007. Improving methods for single-label text categorization. *Instituto Superior Técnico, Portugal* (2007).
[3] Miguel A Carreira-Perpinán and Ramin Raziperchikolaei. 2015. Hashing with binary autoencoders. In *CVPR*. 557–566.
[4] Suthee Chaidaroon and Yi Fang. 2017. Variational Deep Semantic Hashing for Text Documents. In *SIGIR*.
[5] Moses Charikar. 2002. Similarity estimation techniques from rounding algorithms. In *STOC*.
[6] Xi Chen, Yan Duan, Rein Houthooft, John Schulman, Ilya Sutskever, and Pieter Abbeel. 2016. InfoGAN: Interpretable Representation Learning by Information Maximizing Generative Adversarial Nets. *NIPS* (2016).
[7] Bo Dai, Ruiqi Guo, Sanjiv Kumar, Niao He, and Le Song. 2017. Stochastic Generative Hashing. *CoRR* abs/1701.02815 (2017).
[8] Qi Dai, Jianguo Li, Jingdong Wang, and Yu-Gang Jiang. 2016. Binary Optimized Hashing. In *ACM Multimedia*.
[9] Emily L Denton, Soumith Chintala, Rob Fergus, et al. 2015. Deep Generative Image Models using a Laplacian Pyramid of Adversarial Networks. In *NIPS*.
[10] Thanh-Toan Do, Anh-Dzung Doan, and Ngai-Man Cheung. 2016. Learning to Hash with Binary Deep Neural Network. In *ECCV*.
[11] Alexey Dosovitskiy and Thomas Brox. 2016. Generating Images with Perceptual Similarity Metrics based on Deep Networks. In *NIPS*.
[12] Vincent Dumoulin, Ishmael Belghazi, Ben Poole, Alex Lamb, Martín Arjovsky, Olivier Mastropietro, and Aaron C. Courville. 2017. Adversarially Learned Inference. *ICLR* (2017).
[13] Venice Erin Liong, Jiwen Lu, Gang Wang, Pierre Moulin, and Jie Zhou. 2015. Deep hashing for compact binary codes learning. In *CVPR*. 2475–2483.
[14] Aristides Gionis, Piotr Indyk, and Rajeev Motwani. 1999. Similarity Search in High Dimensions via Hashing. In *VLDB*.
[15] Xavier Glorot and Yoshua Bengio. 2010. Understanding the difficulty of training deep feedforward neural networks. In *AISTATS*. 249–256.
[16] Yunchao Gong and Svetlana Lazebnik. 2011. Iterative quantization: A procrustean approach to learning binary codes. In *CVPR*.
[17] Ian Goodfellow, Jean Pouget-Abadie, Mehdi Mirza, Bing Xu, David Warde-Farley, Sherjil Ozair, Aaron Courville, and Yoshua Bengio. 2014. Generative adversarial nets. In *NIPS*. 2672–2680.
[18] Kaiming He, Fang Wen, and Jian Sun. 2013. K-Means Hashing: An Affinity-Preserving Quantization Method for Learning Binary Compact Codes. *CVPR* (2013), 2938–2945.
[19] Kaiming He, Xiangyu Zhang, Shaoqing Ren, and Jian Sun. 2016. Deep residual learning for image recognition. In *CVPR*. 770–778.
[20] Jae-Pil Heo, Youngwoon Lee, Junfeng He, Shih-Fu Chang, and Sung-Eui Yoon. 2012. Spherical hashing. In *CVPR*. IEEE, 2957–2964.
[21] R. Devon Hjelm, Athul Paul Jacob, Tong Che, Kyunghyun Cho, and Yoshua Bengio. 2017. Boundary-Seeking Generative Adversarial Networks. *ArXiv* (2017).
[22] Piotr Indyk and Rajeev Motwani. 1998. Approximate Nearest Neighbors: Towards Removing the Curse of Dimensionality. In *STOC*.
[23] Sergey Ioffe and Christian Szegedy. 2015. Batch Normalization: Accelerating Deep Network Training by Reducing Internal Covariate Shift. In *ICML*.
[24] Herve Jegou, Matthijs Douze, and Cordelia Schmid. 2011. Product quantization for nearest neighbor search. *PAMI* 33, 1 (2011), 117–128.
[25] Diederik Kingma and Jimmy Ba. 2014. Adam: A method for stochastic optimization. *arXiv preprint arXiv:1412.6980* (2014).
[26] Diederik P Kingma and Max Welling. 2013. Auto-encoding variational bayes. *arXiv preprint arXiv:1312.6114* (2013).
[27] Günter Klambauer, Thomas Unterthiner, Andreas Mayr, and Sepp Hochreiter. 2017. Self-Normalizing Neural Networks. In *NIPS*.
[28] Alex Krizhevsky. 2009. Learning Multiple Layers of Features from Tiny Images.
[29] Brian Kulis and Trevor Darrell. 2009. Learning to Hash with Binary Reconstructive Embeddings. In *NIPS*.
[30] Anders Boesen Lindbo Larsen, Søren Kaae Sønderby, Hugo Larochelle, and Ole Winther. 2016. Autoencoding beyond pixels using a learned similarity metric. In *ICML*.
[31] Yann LeCun. 1998. The MNIST database of handwritten digits. *http://yann. lecun. com/exdb/mnist/* (1998).
[32] Qi Li, Zhenan Sun, Ran He, and Tieniu Tan. 2017. Deep Supervised Discrete Hashing. *NIPS* (2017).
[33] Venice Erin Liong, Jiwen Lu, Gang Wang, Pierre Moulin, and Jie Zhou. 2015. Deep hashing for compact binary codes learning. *CVPR* (2015), 2475–2483.
[34] David G Lowe. 1999. Object recognition from local scale-invariant features. In *Computer vision*, Vol. 2. 1150–1157.
[35] Emmanuel Maggiori, Yuliya Tarabalka, Guillaume Charpiat, and Pierre Alliez. 2017. Convolutional neural networks for large-scale remote-sensing image classification. *TGRS* 55, 2 (2017), 645–657.
[36] Xudong Mao, Qing Li, Haoran Xie, Raymond Y.K. Lau, Zhen Wang, and Stephen Paul Smolley. 2016. Least Squares Generative Adversarial Networks.
[37] Sebastian Nowozin, Botond Cseke, and Ryota Tomioka. 2016. f-GAN: Training Generative Neural Samplers using Variational Divergence Minimization. In *NIPS*.
[38] Zhaofan Qiu, Yingwei Pan, Ting Yao, and Tao Mei. 2017. Deep Semantic Hashing with Generative Adversarial Networks. In *SIGIR*.
[39] Ruslan Salakhutdinov and Geoffrey E. Hinton. 2009. Semantic hashing. *Int. J. Approx. Reasoning* 50 (2009), 969–978.
[40] Tim Salimans, Ian J. Goodfellow, Wojciech Zaremba, Vicki Cheung, Alec Radford, and Xi Chen. 2016. Improved Techniques for Training GANs. In *NIPS*.
[41] Fumin Shen, Chunhua Shen, Wei Liu, and Heng Tao Shen. 2015. Supervised Discrete Hashing. *CVPR* (2015), 37–45.
[42] Akash Srivastava, Lazar Valkov, Chris Russell, Michael Gutmann, and Charles Sutton. 2017. VEEGAN: Reducing Mode Collapse in GANs using Implicit Variational Learning. *NIPS* (2017).
[43] Christian Szegedy, Wei Liu, Yangqing Jia, Pierre Sermanet, Scott Reed, Dragomir Anguelov, Dumitru Erhan, Vincent Vanhoucke, and Andrew Rabinovich. 2015. Going deeper with convolutions. In *CVPR*. 1–9.
[44] Christian Szegedy, Vincent Vanhoucke, Sergey Ioffe, Jon Shlens, and Zbigniew Wojna. 2016. Rethinking the inception architecture for computer vision. In *CVPR*.
[45] Ilya Tolstikhin, Sylvain Gelly, Olivier Bousquet, Carl-Johann Simon-Gabriel, and Bernhard Schölkopf. 2017. Adagan: Boosting generative models. *arXiv* (2017).
[46] Jingdong Wang, Ting Zhang, Jingkuan Song, Nicu Sebe, and Heng Tao Shen. 2017. A Survey on Learning to Hash. *PAMI* (2017).
[47] Qifan Wang, Dan Zhang, and Luo Si. 2013. Semantic hashing using tags and topic modeling. In *SIGIR*.
[48] Yair Weiss, Antonio Torralba, and Rob Fergus. 2008. Spectral Hashing. In *NIPS*.
[49] Felix X. Yu, Sanjiv Kumar, Yunchao Gong, and Shih-Fu Chang. 2014. Circulant Binary Embedding. In *ICML*.
[50] Lantao Yu, Weinan Zhang, Jun Wang, and Yong Yu. 2017. SeqGAN: Sequence Generative Adversarial Nets with Policy Gradient. In *AAAI*.
[51] Peichao Zhang, Wei Zhang, Wu-Jun Li, and Minyi Guo. 2014. Supervised hashing with latent factor models. In *SIGIR*.
[52] Ting Zhang, Chao Du, and Jingdong Wang. 2014. Composite Quantization for Approximate Nearest Neighbor Search. In *ICML*.